

Chimia 50 (1996) 199–208  
 © Neue Schweizerische Chemische Gesellschaft  
 ISSN 0009-4293

# Atmospheric Pollution: The Role of Heterogeneous Chemical Reactions

Michel J. Rossi\*

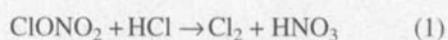
**Abstract.** The chemical kinetics of heterogeneous chemical reactions of importance in the atmosphere are discussed using six examples: 1) water vapor and 2) HCl interacting with ice, 3) ClONO<sub>2</sub> + HCl on ice, 4) HONO + HCl on H<sub>2</sub>SO<sub>4</sub> and ice, 5) HNO<sub>3</sub> reacting on dry CaCO<sub>3</sub> powder and 6) reactions of HNO<sub>3</sub>, N<sub>2</sub>O<sub>5</sub>, ClONO<sub>2</sub>, ClNO<sub>2</sub> on salts such as NaCl and KBr. Quantitative results of uptake coefficients are presented and the importance of ionic displacement reactions at the interface is stressed.

## 1. Introduction

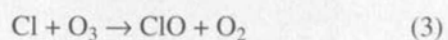
The discovery of the 'ozone hole' atop the Antarctic Continent by Farman and coworkers in 1985 was a shock to the scientific community not only because of the observation of the dramatic depletion of stratospheric ozone but rather because it came as a total surprise which no one had foreseen [1]. The recurrent event may be of rather limited importance with respect to the global stratospheric ozone balance as it is localized in space and time. It is occurring over an uninhabited area for a period of several weeks and does not do any harm to human or animal beings. Its significance lies in the demonstration that even the most inclusive and sophisticated computer models running at that time were unable to 'understand' the newly discovered phenomenon because the chemistry involved was qualitatively incorrect since the models were completely lacking in heterogeneous chemical processes. Up to 1985 significant advances of our understanding of homogeneous gas-phase chemistry had been made such that the scientific community was lulled into the thought that most if not all of stratospheric chemistry was well understood and under control [2]. The occurrence of the ozone hole drew attention to a hitherto neglected area of atmospheric chemistry, namely hetero-

geneous atmospheric chemistry taking place at the interface of the gas and the condensed phase. Even in the three volume assessment of our knowledge of stratospheric ozone, which appeared in 1985, heterogeneous processes received only cursory attention and were deemed to be unimportant in the atmosphere [3].

These heterogeneous processes convert inactive chlorine in the form of reservoir molecules such as HCl and ClONO<sub>2</sub> during the polar night into an active photolyzable form such as HOCl and Cl<sub>2</sub> on the surfaces of tiny frozen atmospheric particulates called polar stratospheric clouds (PSC's) according to the following reactions [4]:

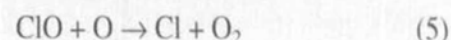
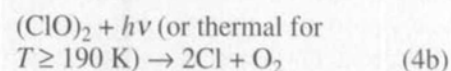


After the polar sunrise the active chlorine-containing molecules Cl<sub>2</sub> and HOCl release atomic Cl through photodissociation and initiate the chain destruction of ozone according to the fast reaction



which is responsible for the fast ozone depletion event taking place in a matter of several days to tens of days. It has become clear that rather unique chemistry is taking place due to the low temperatures of 180–200 K encountered in the lower stratosphere at altitudes between 15 and 25 km atop Antarctica, a fact that is also responsible for the formation of condensed atmospheric particulate on which these in-

terfacial processes can occur. In addition, another unusual chain-propagation step, reaction according to Eqn. 4, is taking place under polar stratospheric conditions. It replaces the 'classical' chain-propagation reaction converting the inactive ClO back to Cl in the global background stratosphere, Eqn. 5 [5]:



In a nutshell, both the heterogeneous chemistry as well as the chain propagation based on the dimer mechanism of ClO conversion to Cl, Eqn. 4, explain the rapid springtime ozone decrease in the polar regions. This explanation has withstood the test of time and is essentially valid today albeit with some important additions such as the participation of bromine-based chemistry [6]. Moreover, some of the heterogeneous atmospheric processes are also occurring elsewhere in the stratosphere and are responsible e.g. for the ozone depletion in the background stratosphere, typically resulting in a 6% decrease of the ozone column per decade in the northern hemisphere, or the occurrence of the spring-time ozone hole above the Arctic, which however is not nearly as pronounced as above Antarctica, both in duration and geographical extent of ozone depletion. Fig. 1 presents two observations as a case in point, one of global ozone decrease (Fig. 1a) and the other of polar ozone decrease (Fig. 1b).

What have we learned from a chemical point of view of these dramatic observations that led us to draw attention to heterogeneous chemical processes? One of the important lessons is that *ionic chemistry* renders these heterogeneous reactions at the interface between the gas and the condensed phase so fast and efficient. Most of the homogeneous chemical reactions taking place as bimolecular or termolecular reactions have small energy barriers resulting in negligible rates at those low temperatures of interest. However, the condensed phase offers the important possibility of ionic reaction mechanisms which are characterized by fast rates down to very low temperatures and which were overlooked by the scientific community in the context of atmospheric chemistry because of lack of precedent. The ozone-hole episode conclusively showed that sophisticated models of atmospheric processes must include the correct chemistry

\*Correspondence: Dr. M.J. Rossi  
 Laboratoire de Pollution Atmosphérique et Sol  
 Département de Génie Rural  
 Ecole Polytechnique Fédérale de Lausanne  
 CH-1015 Lausanne

in order to yield useable and reliable projections of the state of the atmosphere into the future. The global atmosphere is a very complex system of interacting radiative, transport and chemical processes so that the only reliable tool for projections into the future are sophisticated computer models. The question whether or not a measured heterogeneous chemical reaction may or may not be important under atmospheric conditions must be left to the modelers as it is next to impossible to duplicate atmospheric conditions in the laboratory. Most atmospherically relevant densities ( $10^8$ – $10^{10}$  molecules  $\text{cm}^{-3}$ ) and the associated time scales (days to weeks) are difficult to achieve under laboratory conditions. Therefore, we adopted the strategy to first *study the chemical mechanism* in order to enable reliable extrapolation of the kinetics to atmospheric conditions, assuming that the mechanism does not change within a factor of 100 or so in variation of reactant density.

Today the polar and background ozone decrease is understood as one possible manifestation of the *increase of atmospheric trace gases* due to human activities. The observed ozone decrease is directly linked to the increasing chlorine load of the atmosphere, primarily in the form of chlorofluorocarbon (CFC's) source gases transforming into reservoir (= inactive) gases such as HCl and  $\text{ClONO}_2$  [7]. Some of the other consequences of the change in atmospheric trace-gas composition are the greenhouse effect

which has to do with the increase of IR-absorbing gases in the lower atmosphere (troposphere) such as  $\text{CO}_2$ ,  $\text{CH}_4$ , CFC's and related compounds (hydrofluorocarbons (HFC's), hydrofluorochlorocarbons (HCFC's)),  $\text{N}_2\text{O}$  and tropospheric (surface) ozone. The latter gas is especially difficult to treat as its increase depends on global emission scenarios of  $\text{NO}_x$  and hydrocarbons which are both linked to the future production and use of energy and projected industrial activity.

Atmospheric 'anomalies' such as acid rain and photochemical smog are well known nuisances to humans adversely affecting the air quality [8]. In the case of acid rain  $\text{SO}_2$  is known to be the source gas, and with successful abatement strategies to control the emission of  $\text{SO}_2$  in place the acid-rain problem has been significantly reduced in many parts of the industrialized world in the last ten years. The photochemical smog problem is intimately connected to the presence of  $\text{NO}_x$  and hydrocarbons, in part of natural, and in part of anthropogenic (= manmade) origin. To date many urban areas are plagued by smog, especially under stagnant meteorological conditions in summer, and significant efforts are undertaken in order to control the emission of the primary source gases. The formation of smog is controlled by four factors:  $\text{NO}_x$ , hydrocarbons, the availability of sunlight and temperatures in excess of  $18^\circ$  thus sustaining a dark flame wherein the hydrocarbon fuel is burnt in the presence of  $\text{NO}_x$  as the

catalyst and where the chain carriers, mainly OH and  $\text{HO}_2$ , are generated through photolysis. In this case the abatement strategy is more difficult to design because it depends on a combination of measures. In Switzerland the most promising strategy seems to limit the  $\text{NO}_x$  emissions which may be obtained by equipping all motor vehicles with catalytic converters as 75% of the  $\text{NO}_x$  emissions seem to originate from this source [9].

In a similar manner the emission of jet aircraft and its effects on the atmosphere are presently an intense field of study [10]. It seems that the injection of  $\text{NO}_x$  and other combustion products such as  $\text{H}_2\text{O}$  which is responsible for the formation of the visible contrails at temperatures  $\leq -40^\circ$ ,  $\text{SO}_2$ , soot and other species into the atmospheric layer around the tropopause of 8–15 km of altitude may cause important changes in the protective stratospheric ozone layer. The quantitative change of stratospheric ozone depends very sensitively on flight altitude and on the chemistry model used for assessment. The corollary is that for all the atmospheric effects presented in the last paragraphs heterogeneous processes are suspected to be important, and ongoing research is centered on the discovery of important new interfacial processes. In this presentation we will place the emphasis on work that has been performed in our laboratories at the Laboratoire de Pollution Atmosphérique et Sol (LPAS) of the EPFL in the last four years.

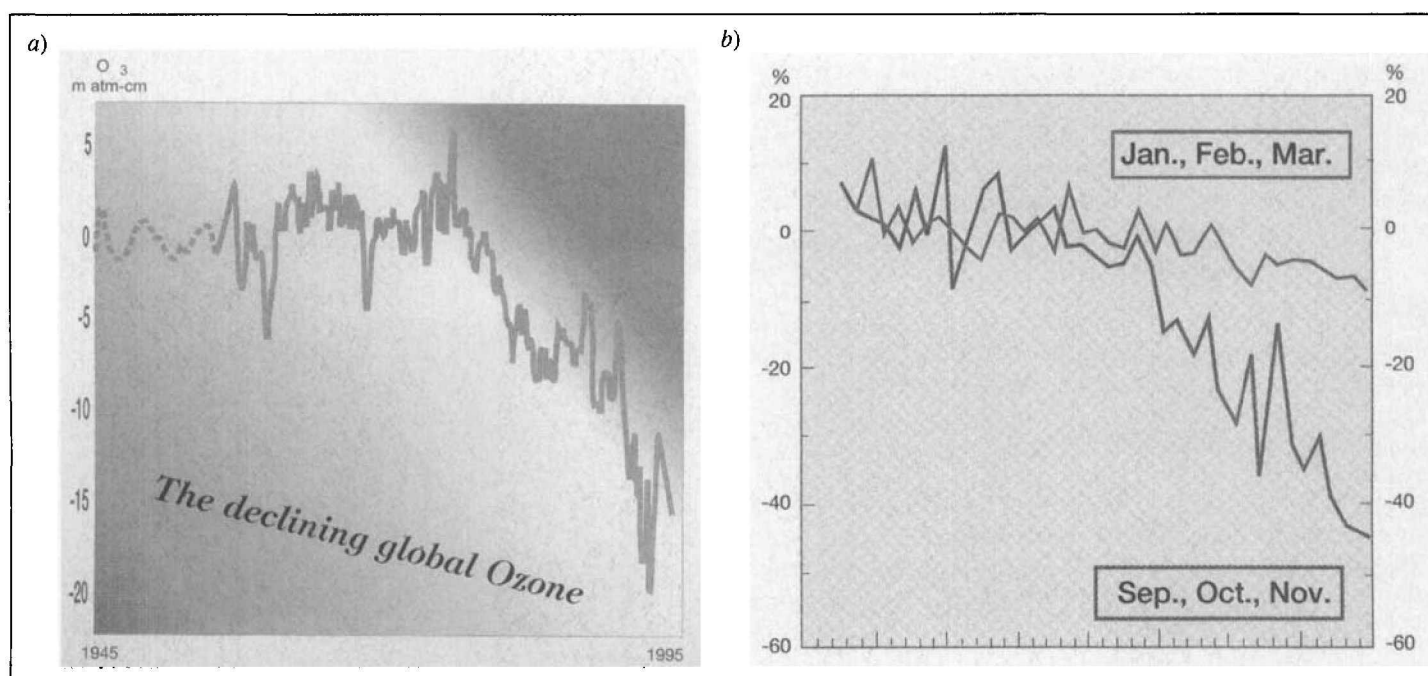


Fig. 1. a) Time series of the decrease of the global total ozone column in milliatm-cm (= 1 Dobson unit) from 1945 to 1995. The variations superimposed on the general decline are regular oscillations in total ozone such as the quasibiennial (~two year) oscillation and the 11 year solar-cycle variation. b) Ozone seasonal deviations averaged over 1985–1994 from pre-ozone hole (1957–1978) averages in the Antarctic. Summary for stations Faraday, Syowa, Halley Bay, South Pole.

## 2. Experimental Apparatus

The majority of the experimental investigations were performed in a low-pressure reactor or *Knudsen* cell which was part of a flowing gas experiment. The low pressure of typically 1 mTorr, give or take an order of magnitude (1 mTorr corresponds to a density of  $3.21 \times 10^{13}$  molecules  $\text{cm}^{-3}$  at 300 K), affords molecular flow conditions such that each molecule preferentially undergoes wall collisions rather than collisions with other molecules in the gas phase. The molecular flow regime, therefore, enables the molecules to diffuse to the surface of interest at their molecular velocity thus making surface processes the rate-limiting step rather than diffusion which may become rate-limiting at higher total pressures [11].

The molecules enter the *Knudsen* cell and effuse out of an escape orifice after they have spent a certain amount of time, the lifetime  $\tau$ , inside the reactor during which they underwent several thousand collisions with the wall. The inverse of  $\tau$  is  $k_c$ , the escape rate constant, and depends only on the molecular velocity as well as on the geometry of the reactor:

$$1/\tau = k_c = (\{c\}/4V) \cdot A_h \quad (6)$$

where  $\{c\}$  is the average molecular velocity with which the molecules actually move inside the cell in the molecular flow regime,  $V$  and  $A_h$  are the volume and the area of the escape orifice, respectively. Values for  $k_c$  are on the order of one second, give or take an order of magnitude for the reactor geometries used. At a constant flow of molecules into the reactor giving rise to a steady-state partial pressure, the average molecule is lost through physical pumping across the escape orifice. The molecules effusing out of the orifice are forming an effusive (thermal) molecular beam which is monitored using electron-impact mass spectrometry. The goal of the measurement is to determine a rate constant for chemical loss of a given molecule on a surface of interest. To this end a part of the reactor wall is replaced by the surface of interest which is often placed in a second (sample) chamber which can be isolated from the *Knudsen* reactor (reference) by a gas-tight plunger or isolation stopcock. Upon opening of the isolation plunger the steady-state pressure drops to a lower value if the molecule interacts with the surface. It is thus irreversibly removed from the gas phase. This 'chemical' loss of interest is a competitive pathway to ordinary 'physical' loss by effusion across the escape aperture and is measured relative to the escape rate. The rate constant  $k_c$  is, therefore, the 'yardstick' for the measurement of the rate constant of interest,  $k_h$ . Simple steady-state considerations lead to the following expression for  $k_h$  assuming that the rate law for heterogeneous interaction is first order in the molecular density or pressure:

$$k_h = ((S_0 - S)/S)k_c \quad (7)$$

where  $S_0$  and  $S$  correspond to the mass-spectrometric signal with the sample isolated (no heterogeneous interaction) and exposed to the gas flow, respectively. Eqn. 7 demonstrates that the relative measurement of  $S_0$  and  $S$  corresponding to active surface 'off' and 'on' is put on an absolute basis using  $k_c$  thus leading to an absolute measurement of  $k_h$  [12].

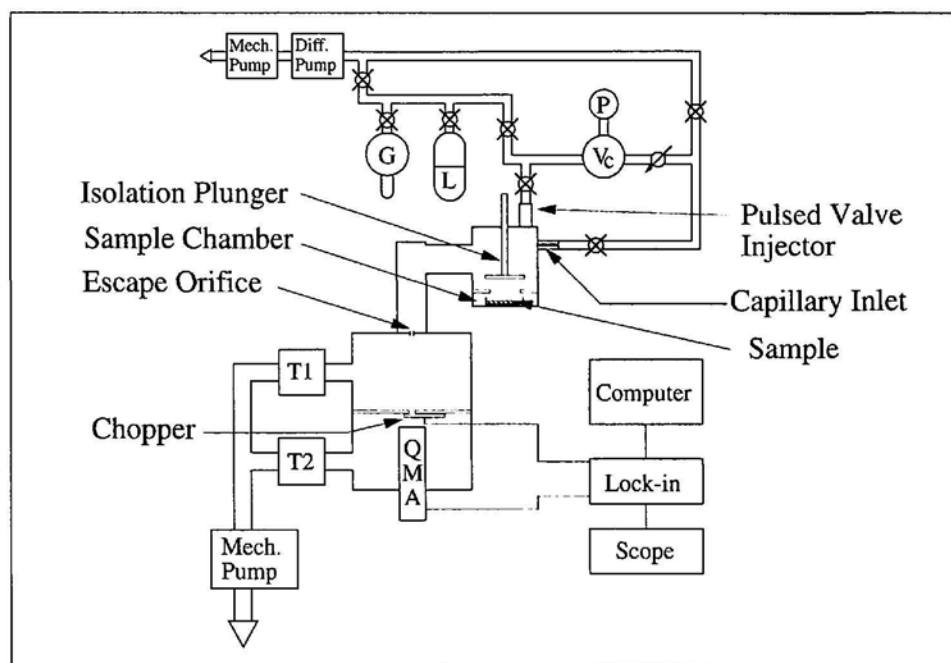


Fig. 2. Schematic view of low-pressure flow reactor (*Knudsen* cell) sitting on top of the vacuum chambers the lower of which houses the molecular-beam-modulated electron-impact mass spectrometer (QMA)

The values of  $k_h$  obtained from experiment may be expressed on a per collision basis leading to uptake coefficients  $\gamma$  which correspond to the probability that a molecule interacting with a surface stays adsorbed on it and is, therefore, removed from the gas phase. The uptake coefficient is calculated according to:

$$\gamma = k_h / \omega = 4Vk_h / \{c\}A_s \quad (8)$$

where  $\omega$  is the gas-surface collision frequency of the molecule with the surface of interest of area  $A_s$ . The uptake coefficient describes the net uptake corresponding to the difference between adsorption and desorption rate. The range of uptake coefficients that are accessible to measurement using our *Knudsen* cell approach lies in the range  $10^{-6} \leq \gamma \leq 1.0$ . This large dynamic range in the measurement of  $\gamma$  is made possible by changing  $A_h$  by two orders of magnitude thus changing the yardstick or meter against which  $k_h$  is measured.

It is also important to note that we are exposing the gas to *model* surfaces whose overall bulk chemical composition is identical to or at least comes very close to the one of atmospheric particulates such as combustion aerosols (soot), ice crystals and  $\text{H}_2\text{SO}_4$  aerosol of various composition. For studies where the substrate has to be kept at low temperatures such as for kinetic studies involving ice and other frozen surfaces a special low-temperature sample holder has been constructed. The sample is placed into a copper dish that is in contact with a heat exchanger which is alternatively cooled by circulating cold air and resistively heated using a double-loop temperature controller. A design has been chosen which maximizes the gradient between the cold temperature-controlled surface and the rest of the *Knudsen* reactor remaining at ambient temperature. A similar design has been chosen for a high-temperature sample support which enables the heating of samples up to temperatures of 500 K.

Fig. 2 displays an overview of the two-chamber *Knudsen* reactor with which we have per-

formed most of the measurements described below. In addition to molecular-beam-modulated mass spectrometry we have used real-time *in situ* optical diagnostics based on pulsed laser excitation such as laser-induced fluorescence (LIF) and Resonance-Enhanced Multiphoton Ionization (REMPI). To this end the *Knudsen* cell displayed in Fig. 2 was equipped with a set of optical windows to allow pulsed laser excitation and photon detection. This dual diagnostic capability enables us to calibrate the optical signals in terms of absolute density using the mass spectrometer. We believe it to be necessary to know the absolute concentrations of the reactants when studying heterogeneous kinetics because most mechanisms turn out to be complex [11].

We have recently developed an additional real-time kinetic technique based on the *Knudsen* cell which involves pulsed admission of molecules interacting with easily saturable surfaces such as soot, salt and ices. A known number of gas molecules are admitted by a pulsed solenoid valve into the reactor and interact with the active surface. The decay of the gas burst is followed in real time using time-dependent mass spectrometry. In the case of a measurable heterogeneous interaction the lifetime of the molecule will be shortened as the time-dependent signal will decay faster in the presence of the active surface according to the relation:

$$S = S_0 \exp(-(k_c + k_h)t) \quad (9)$$

This technique has two important advantages over the traditional steady-state technique: *a*) it affords the separation between the kinetics of the adsorption and desorption step because there are no molecules on the surface at  $t=0$  which are able to desorb, and *b*) it keeps the dose to a minimum thereby avoiding surface saturation and contamination phenomena. A typical lower limit for a gas burst is in the range of 2% of a formal monolayer, depending somewhat on the identity of the molecule. In any case, we do not expect any measurable saturation effect at surface coverages

of a few percent of a formal monolayer. Finally, it has to be pointed out as well that the experimental effort also includes a fair amount of preparative work as compounds such as  $N_2O_5$ ,  $ClONO_2$ ,  $BrONO_2$ ,  $CINO_2$ ,  $HONO$ ,  $NOBr$  and others have to be synthesized and purified shortly before their use in view of their limited thermal stability.

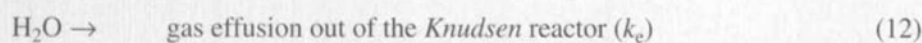
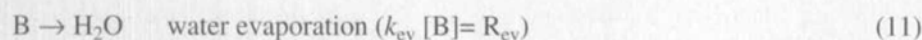
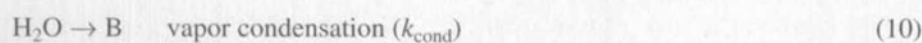
### 3. Representative Results and Discussion

In what follows we will briefly present some representative examples of studies of heterogeneous reactions performed at EPFL over the last four years emphasizing both the fundamental aspects of the chemical kinetic studies as well as their atmospheric implications.

#### 3.1. The Interaction of Water Vapor with Ice

The condensation and evaporation of  $H_2O$  vapor on its own solid (ice, snow) and fluid condensed phase is one of the most important processes in the atmosphere. Although the vapor pressure of  $H_2O$  over liquid water and ice is well known from experiments down to 170 K the kinetics of condensation and evaporation was the subject of many studies over the years [13]. The measurement of the vapor pressure, which is a thermodynamic quantity and corresponds to an equilibrium constant, says nothing about the kinetics of the individual condensation and evaporation process for which experimental results cast in the form of evaporation and condensation coefficients vary up to a factor of 200 depending on the experimental technique and the temperature [14]. We embarked on a program to experimentally determine this simplest of systems in order to measure a reference reaction against which all others may be compared to.

The simplest experiment consisted of measuring the  $H_2O$  vapor effusing out of the *Knudsen* cell in the presence of ice in the temperature range 160–220 K according to the following simple kinetic scheme involving  $H_2O$  vapor and bulk ice, B:



where  $k_{\text{cond}}$  and  $k_c$  correspond to the condensation and escape rate constant, respectively, and  $R_{\text{ev}}$  equals the rate of evaporation in molecules  $s^{-1}$ . The experimentally observed vapor pressure is a steady-state

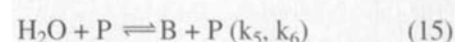
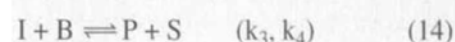
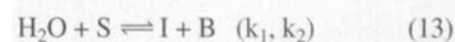
vapor pressure and is not equal to its equilibrium value because it is perturbed by the reaction according to *Eqn. 12*. However, it is possible to calculate the equilibrium vapor pressure by separately determining  $k_c$  and  $R_{\text{ev}}$ . By obtaining two independent data sets corresponding to *Knudsen* reactors with two different escape orifices we may obtain the desired parameters. *Fig. 3* presents an *Arrhenius* plot of  $k_{\text{cond}}$  as a function of inverse temperature in the range 160–220 K. By dividing the values of  $k_{\text{cond}}$  by  $\omega = 150 s^{-1}$  one obtains the condensation coefficient as a function of temperature which varies between 0.05 and 0.5.

The measured negative activation energy for  $k_{\text{cond}}$  of  $-3.0 \pm 1.5$  kcal/mol suggests kinetic complications and points towards a complex mechanism, a fact that is surprising for such a simple physical system. The numerical values of the evaporation rates of  $H_2O$  from an ice surface are impressive even at low temperatures:  $R_{\text{ev}}$  corresponds to the evaporation of 10 monolayers of  $H_2O$  per s at 180 K and to 80 monolayers at 200 K. These high values for  $R_{\text{ev}}$  reveal the dynamic nature of an ice surface even at low temperatures which has important consequences for the condensation of less volatile molecules on ice surfaces. A short time after a heavy molecule has 'landed' on an ice surface it is 'buried' and incorporated into the bulk of the ice by the rapid evaporation and condensation of  $H_2O$ .

In view of the suspected complexities of this simple reaction we performed additional kinetic experiments in real time admitting bursts of water vapor into the *Knudsen* reactor and observing the subsequent decay of the  $H_2O$  pulse. Surprisingly,  $k_h$  (*Eqn. 9*) was found to be a function of the dose. The measured values for  $k_h$  are displayed in *Fig. 4* for an ice surface at 180 K. This dependence of  $k_h$  on the dose of  $H_2O$  is a subtle effect and corresponds to an increase of  $k_h$  by at most a factor of six over almost a three order of magnitude variation in dose. The dose corresponding to a nominal monolayer of  $H_2O$  on ice is on the

200 K whereas it is not observed at 160 K. The interpretation of these results necessitates chemical kinetic modeling because of the incidence of a pressure-dependent mechanism.

The simplest mechanism which explains both our steady-state as well as the pulsed valve experiments involves the competition between a *Langmuir-Hinshelwood*-type condensation process and an autocatalytic process whose rate is depending upon the  $H_2O$  pressure [15]. It is given by the following reversible equations:



where S is a nominal surface site for  $H_2O$  condensation and I and P are two intermediate states which correspond to adsorbed  $H_2O$  molecules. Each  $H_2O$  molecule is surrounded by four others in bulk ice whose lattice corresponds to a distorted diamond structure, thus forming four H-bonds with neighboring  $H_2O$  molecules. The various species in the model differ in the number of 'free valences', that is the ability to engage in H-bond formation up to the maximum coordination number of four.  $H_2O$  has four free valences, each following species has one valence less ( $I = 3$ ,  $P = 2$ ,  $S = 1$  and  $B = 0$ ). When  $H_2O$  is forming one H-bond to S it itself becomes an I molecule with one H-bond and three free valences thereby converting the original S state to a B state (*Eqn. 13*). The reverse process of breaking a H-bond is also possible and is embodied in the reaction according to *Eqn. 14* where B is split into two S states, one of which forms a H-bond with I thus becoming a P state. Finally,  $H_2O$  may directly form two H-bonds at once in a concerted fashion thereby transforming a P state into a B state and at the same time becoming a P state (*Eqn. 15*). The reaction corresponding to *Eqn. 15* seems to be essential and is in fact *autocatalytic* in P thus preserving the density of catalytic P states which are necessary for the increase of the rate of  $H_2O$  adsorption at increasing pressure.

The increase of the condensation coefficient with increasing pressure essentially results from the increased coverage of P at increasing pressure and may help explain the fact of the large range of experimental values obtained to date [14]. The model reproduces both the observed negative temperature dependence of  $k_{\text{cond}}$  (*Fig. 3*) as well as the dose dependence (*Fig. 4*). The significance of the kinetic work, how-

order of  $10^{16}$  molecules. *Fig. 4* displays thus a dose dependence ranging from less than 10% of a nominal monolayer per pulse to more than 400 monolayers. This dose dependence is more pronounced at

ever, lies in the fact that they require a mechanism dealing with at least *two additional kinetically distinguishable species* in going from the simple mechanism, *Eqns. 10 and 11*, to the more complex one given by *Eqns. 13–15*.

### 3.2. The Interaction of HCl with Ice

HCl is a stable chlorine-containing reservoir molecule which plays a pivotal role in the chemistry of the polar stratosphere. Together with the slightly more reactive ClONO<sub>2</sub> whose heterogeneous reactivity will be discussed below, it constitutes the main chlorine-containing species throughout the stratosphere, and the sum of both HCl and ClONO<sub>2</sub> attains values on the order of 2–3 ppb. In view of the strong bond of 103 kcal/mol and the UV absorption spectrum of HCl it was believed that once chlorine was transformed into HCl, mainly by abstraction of an H-atom from CH<sub>4</sub> by HCl, it would be removed from the catalytic ozone-destruction cycle. However, it was shown that chlorine in HCl could be activated efficiently in a heterogeneous reaction following *Eqn. 1* meaning it could be transformed into another chlorine-containing molecule which would readily release atomic chlorine upon photolysis. The reaction given by *Eqn. 1* is very popular amongst atmospheric modelers because it kills two birds with one stone by converting the chlorine of *two* reservoirs into the active form Cl<sub>2</sub> releasing two active Cl-atoms upon photolysis.

It is well known from general chemistry that HCl is very soluble in liquid H<sub>2</sub>O but scarcely so in ice. The known phase diagram of HCl/H<sub>2</sub>O reveals a coexistence line between fairly concentrated HCl solutions and 'ice' in the temperature range between 220 and 180 K which is of interest in the context of stratospheric chemistry (*Fig. 5*) [16]. However, in the pertinent pressure range of 10<sup>-7</sup> Torr HCl does not form a stable fluid phase atop the ice and the system is better described as bulk ice contaminated by small amounts of adsorbed HCl.

In order to study the uptake kinetics of HCl on ice we performed pulsed valve experiments of HCl on ice and were able to conclude that at doses corresponding to even less than a nominal monolayer HCl is rapidly forming a fluid layer on the ice thus facilitating further dissolution of gas phase HCl into the fluid condensed phase [17]. Such a pulse of HCl results in a rapid decay of the gas-phase HCl density corresponding to *k<sub>h</sub>* values of 30 s<sup>-1</sup> at 170 K and 5 s<sup>-1</sup> at 210 K reflecting the high solubility of HCl in the liquid layer created by its own pulse. After the decay of the pulse a

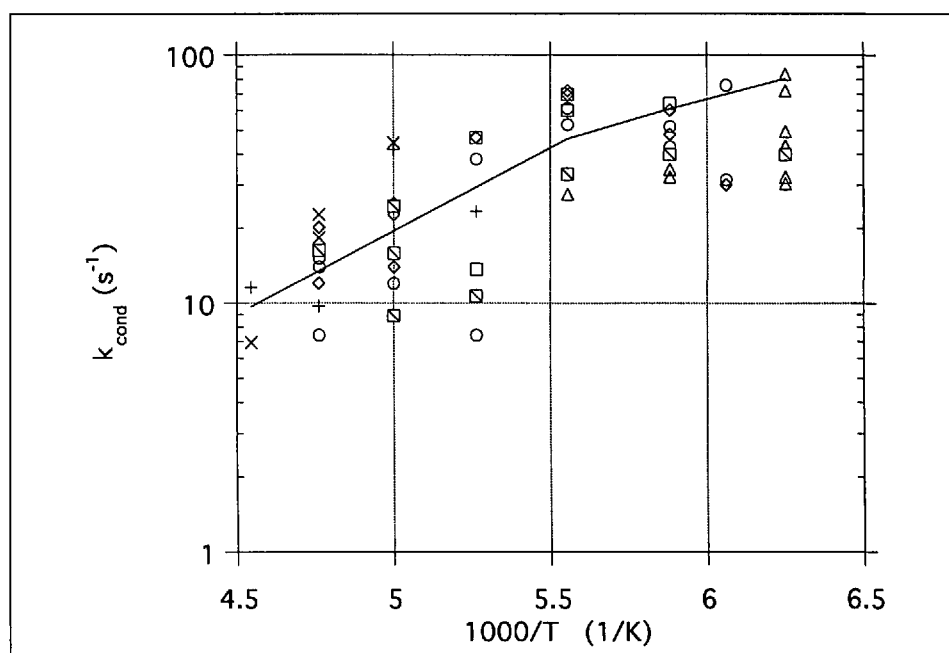


Fig. 3. Arrhenius plot of the rate constant  $k_{cond}$  for the condensation of H<sub>2</sub>O on ice under near-equilibrium conditions in the temperature range 160–220 K. The Knudsen reactor had the following characteristics:  $V = 1.18 \text{ dm}^3$ , area of the active surface =  $11.3 \text{ cm}^2$ ,  $k_c(\text{H}_2\text{O}) = 1.0$  (small aperture) and  $7.5$  (large aperture) s<sup>-1</sup>,  $\omega = 150 \text{ s}^{-1}$ .

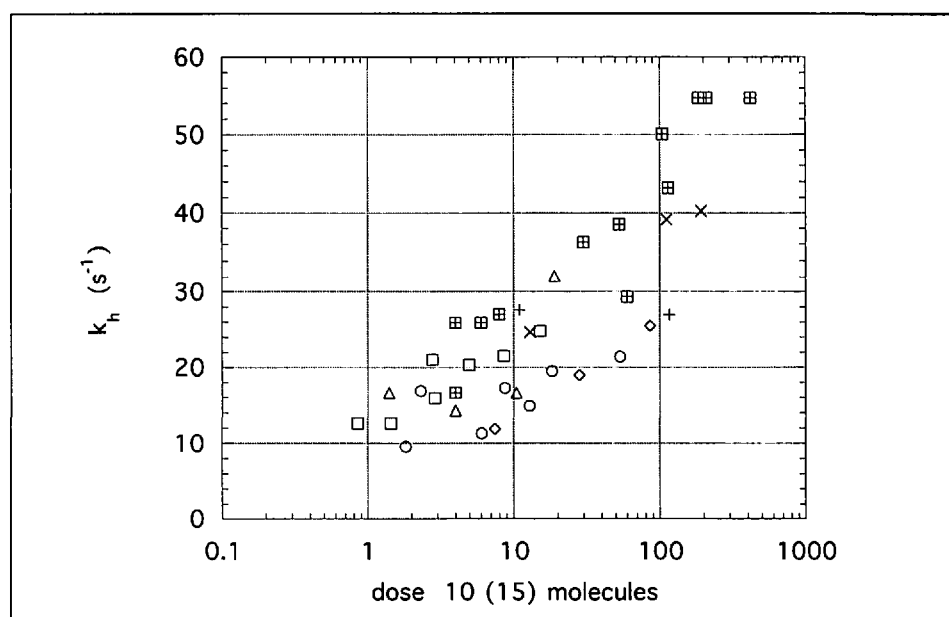


Fig. 4. Dependence of the decay time constant  $k_h$  of a H<sub>2</sub>O pulse admitted to the Knudsen cell in the presence of ice at 180 K as a function of the dose (number of H<sub>2</sub>O molecules in the pulse). The different symbols pertain to different experiments, and the Knudsen reactor parameters are the ones from *Fig. 3*.

steady-state HCl partial pressure is maintained in the Knudsen cell which agrees with the equilibrium vapor pressure of Molina and coworkers at the liquid-solid coexistence line [18] (*Fig. 5*). This steady-state signal persists for a certain time depending on the dose and drops to zero after the supply of HCl from the surface is exhausted.

The mass balance reveals that most of the HCl is retained by the ice sample. In view of the dynamic nature of the interface this can be expected as many of the molecules are 'buried' in the bulk of the pure

ice never again to desorb. The fact that even doses corresponding to less than a nominal HCl monolayer lead to a well defined HCl equilibrium vapor pressure predicted by the HCl/H<sub>2</sub>O phase diagram can be interpreted that localized 'patches' or 'potholes' of HCl/H<sub>2</sub>O fluid form on the ice surface. Apparently, the formation of a macroscopic fluid layer is not necessary to maintain an equilibrium HCl vapor pressure.

If, on the other hand, the dose or the flow rate falls below a certain limit in pulsed and steady-state experiments, re-

spectively,  $k_n$  drops to values comparable to  $k_c$  in pulsed valve experiments and the steady-state uptake drops to unmeasurably low values. This threshold may be interpreted that the formation of the liquid HCl/H<sub>2</sub>O layer on the ice surface is enabled by a minimum-required impact rate which probably must exceed the evaporation rate of H<sub>2</sub>O of the ice surface. It thus follows that this threshold value for the impact rate expressed as the number of HCl molecules striking 1 cm<sup>2</sup> of the ice surface in unit time largely depends on the temperature and is in fact equivalent to a pressure barrier for dissolution of HCl in ice.

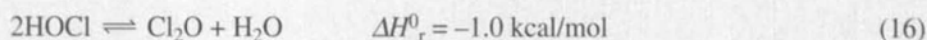
We may conclude that HCl only scarcely dissolves in pure ice at stratospheric conditions in view of the HCl partial pressures on the order of 10<sup>-7</sup>–10<sup>-6</sup> at temperatures between 180 and 220 K. The physical state of HCl under those conditions corresponds to an impurity adsorbed along grain boundaries or hairline cracks within the ice sample. On the other hand no change in physical behavior of the HCl/H<sub>2</sub>O system has been observed in going from an ice sample deposited from the vapor phase at 160 K to one generated from freezing a sample of distilled H<sub>2</sub>O after several freeze-pump-thaw cycles. This may well mean that the natural surface roughness of the ice adsorbs and retains a certain quantity of HCl.

### 3.3. The Interaction of ClONO<sub>2</sub> with HCl and Ice

The discovery in the early seventies of ClONO<sub>2</sub> in the atmosphere and its mechanism of formation by recombination from ClO + NO<sub>2</sub> caused a false sense of security amongst the atmospheric science community. The reasoning followed the hypothesis that the formation of an inactive reservoir such as ClONO<sub>2</sub> which has a small actinic absorption cross section and which is generated from two free radicals participating in catalytic ozone-destruction cycles, removed the immediate threat of massive ozone destruction. However, it later turned out that this expectation was a fallacy because heterogeneous pathways of activation of ClONO<sub>2</sub> had not been taken into account. In view of the importance of the reactions corresponding to Eqns. 1 and 2 for the chlorine activation scenario we will briefly present some of the fundamental processes of heterogeneous chemistry.

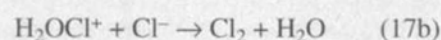
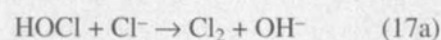
Fig. 6 displays a typical steady-state experiment, wherein a bulk ice sample at 180 K is exposed to a steady flow of ClONO<sub>2</sub> of 10<sup>14</sup> molecules s<sup>-1</sup> monitored at  $m/e = 46$  (NO<sub>2</sub><sup>+</sup>). Upon exposing the ice

sample the signal  $m/e$  at 46 rapidly drops corresponding to an initial value of  $\gamma = 0.3$  for ClONO<sub>2</sub> uptake by ice. Subsequently, the signal gradually rises again due to a rapid saturation process on ice and eventually reaches a steady-state level. The rate of formation of HOCl monitored at  $m/e = 52$  (HOCl<sup>+</sup>) is slowly rising after an initial burst and reaches also a steady-state level similar to the ClONO<sub>2</sub> signal. At higher flow rates of ClONO<sub>2</sub>, Cl<sub>2</sub>O is accompanying the formation of HOCl. It is the formal anhydride of HOCl and is thermodynamically favored by 1 kcal/mol in equilibrium (Eqn. 16) [19]:



In separate reference experiments we established that the HOCl interaction with water ice and HNO<sub>3</sub>-exposed water ice is negligible at our used flow rates. Moreover, no Cl<sub>2</sub>O formation could be observed using HOCl as the precursor so that we conclude that it is a secondary product formed at higher flow rates of ClONO<sub>2</sub>.

From the difference in the rate of ClONO<sub>2</sub> uptake and the rate of appearance of the primary product HOCl, which is especially apparent at higher ClONO<sub>2</sub> flow rates, it is clear that an intermediate which is slowly releasing HOCl is generated at the interface. Sodeau and coworkers identified an unusual intermediate resulting from ClONO<sub>2</sub> exposure to their ultrathin ice samples and attributed it to H<sub>2</sub>OCl<sup>+</sup>...NO<sub>3</sub><sup>-</sup> based on its IR-absorption spectrum [20]. This species corresponds to protonated hypochloric acid stabilized by nitrate ion and represents an HOCl precursor. We assume that the intermediate in our case is identical to that found by Sodeau even though our experimental conditions differ significantly from theirs. When we 'interrogate' our ice sample that was previously exposed to ClONO<sub>2</sub> by exposing it to an excess flow of HCl we observe to our surprise only spurious amounts of Cl<sub>2</sub> [21]. We expected quantitative conversion of HOCl or its precursor, protonated hypochloric acid, H<sub>2</sub>OCl<sup>+</sup>, with HCl according to the fast reactions of Eqns. 17a and 17b:



Apparently, the HOCl precursor is completely unreactive towards displacement of OH<sup>-</sup> by Cl<sup>-</sup> (Eqn. 17b), perhaps because of the limited kinetic activity of H<sub>2</sub>O as a leaving group in nucleophilic displacements.

Pulsed valve experiments of ClONO<sub>2</sub> interacting with ice indicate an extreme sensitivity of the reaction corresponding to Eqn. 2 to surface saturation, presumably due to the accumulation of stable HNO<sub>3</sub> hydrates that form when HOCl is liberated according to Eqn. 2 [21]. A pertinent observation is the fact that no saturation of ClONO<sub>2</sub> uptake is observed when a simultaneous flow of ClONO<sub>2</sub> and NH<sub>3</sub> is brought to interact with the ice sample suggesting a rapid destruction of the HOCl precursor by NH<sub>3</sub>. A large sustained uptake of ClONO<sub>2</sub> is observed whereas HOCl is not because it is neutralized by NH<sub>3</sub> so

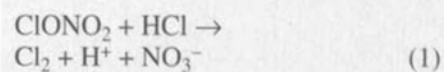
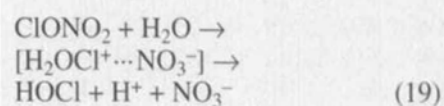
result in NH<sub>4</sub>OCl. On the other hand, a high rate of Cl<sub>2</sub>O formation is also observed indicating that it results from a facile secondary nucleophilic displacement, Eqn. 18:



where ClO<sup>-</sup> represents the reactive part of gas-phase ClONO<sub>2</sub> interacting with HOCl. In addition, gas-phase HOCl also reacts with the same precursor according to Eqn. 18.

If on the other hand the ice sample is exposed first to HCl and subsequently to ClONO<sub>2</sub>, Cl<sub>2</sub> is seen to rise promptly and quantitatively as a result of the reaction given by Eqn. 17. Figs. 7a and 7b present a good example for the determination of  $k_n$  for the decay of a pulse of ClONO<sub>2</sub> in the presence of ice and the correlated rise of Cl<sub>2</sub> on the same time scale, thus emphasizing the prompt mode of Cl<sub>2</sub> compared to HOCl formation (in the absence of HCl).

From a mechanistic point of view both HCl and H<sub>2</sub>O are competing for reaction with ClONO<sub>2</sub> according to Eqns. 19 and 1:



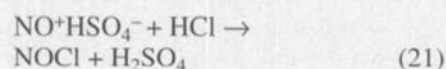
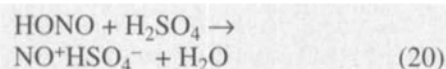
where the spontaneous decomposition of the HOCl precursor in the reaction according to Eqn. 19 may be accelerated by a base such as NH<sub>3</sub>. As an important corollary we note that Cl(+1) in the HOCl precursor is not titratable by Cl(-1) whereas formation of the secondary product Cl<sub>2</sub>O by nucleophilic displacement with ClO<sup>-</sup> seems facile (Eqn. 18).

These few kinetic facts may have ramifications for atmospheric chemistry. For one, the sequence of interaction of ClO-

NO<sub>2</sub> and HCl with ice certainly matters as our sequential exposure experiments have shown. For instance the conclusion reached by some authors that the reaction following Eqn. 1 occurs first through the reaction according to Eqn. 2 with subsequent fast titration by HCl according to Eqn. 17b needs careful reexamination for the case of an ice substrate [19][22]. The reactivity of ClONO<sub>2</sub> has to be seen in terms of two competitive reactions, one slow through the HOCl precursor (Eqn. 19), the other one rapid by way of a direct reaction (Eqn. 1) involving Cl<sup>-</sup> in a mobile phase. Our results point towards the importance of nucleophilic displacement reactions and ionic mechanisms.

### 3.4. The Heterogeneous Interaction of HONO and HCl

Burley and Johnston recently presented an interesting hypothesis according to which HCl may be activated by HONO using H<sub>2</sub>SO<sub>4</sub> as a catalyst following Eqns. 20 and 21 [23]:



The N(+3) species is effectively dissolved in H<sub>2</sub>SO<sub>4</sub> as nitrosylsulfuric acid (NSA) which is stable at H<sub>2</sub>SO<sub>4</sub> concentrations exceeding 72% by weight at ambient temperature. Below this concentration HONO is dissolved in molecular (undissociated) form although the stability range of NSA may be extended to more dilute solutions with decreasing temperature. The reason for the interest in this reaction is the hypothesis that the exhaust from commercial and military jet aircraft flying at heights corresponding to both just above and below the tropopause may affect the stratospheric ozone layer by activating HCl into readily photolyzable NOCl. Aircraft exhaust with its emission of H<sub>2</sub>O, NO, SO<sub>2</sub>, soot particles and many other reactive species represents a very reactive environment for heterogeneous reactions in which background gases such as HCl may also actively participate [10].

We devised a two-pronged approach to consider this atmospheric question [24]: First, we intended to study the uptake of gas-phase HONO on H<sub>2</sub>SO<sub>4</sub> in order to see if NSA was indeed generated at all. The second step consisted of investigating the activation reaction according to Eqn. 21 of HCl on NSA. Fig. 8 displays the results of the uptake coefficients  $\gamma$  of HONO on aqueous solutions of H<sub>2</sub>SO<sub>4</sub> of variable

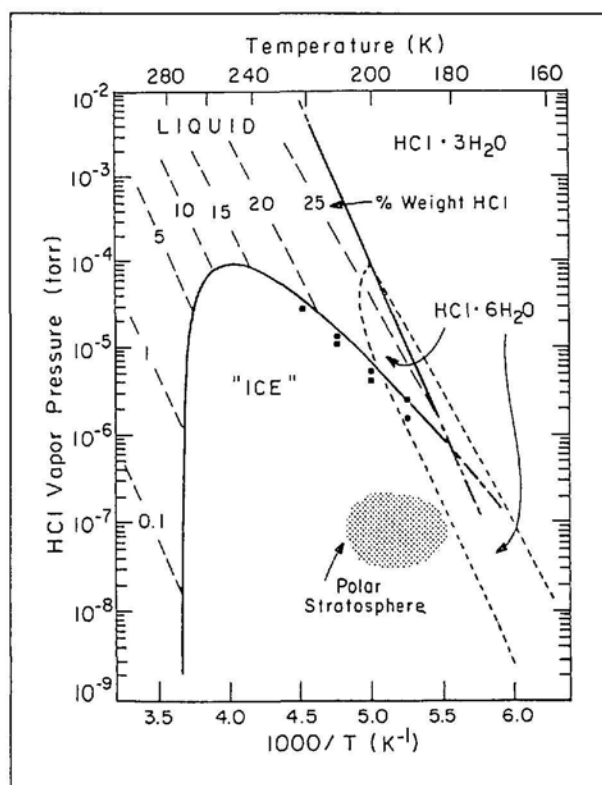


Fig. 5. Phase diagram for the HCl/H<sub>2</sub>O system. The equilibrium vapor pressure of HCl determined from pulsed HCl dosing experiments in several different Knudsen reactors follow the line established in equilibrium experiments by Molina and coworkers [18]. Two independent data sets were used to calculate the equilibrium vapor pressure (● combination of 8- and 15-mm-diameter, ■ combination of 4- and 8-mm-diameter-aperture Knudsen reactor).

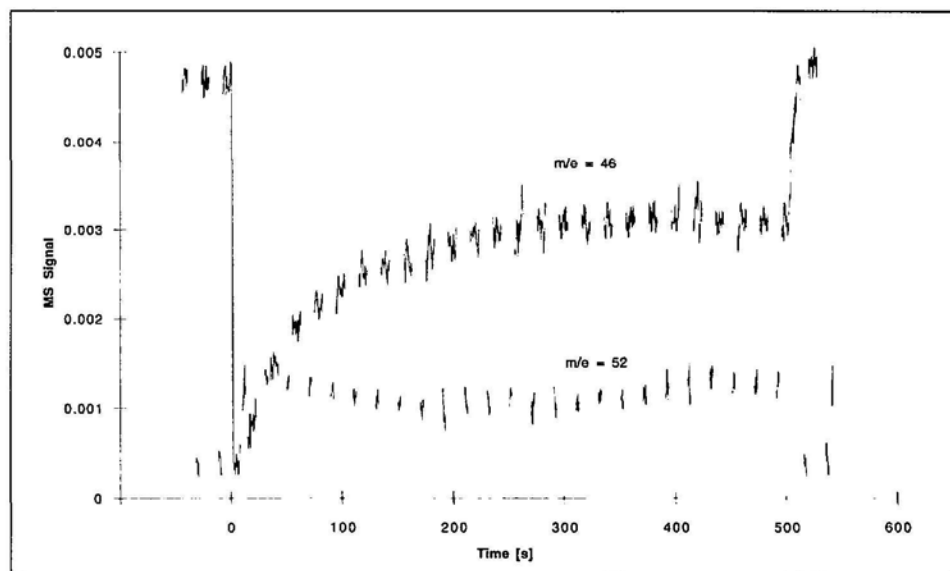


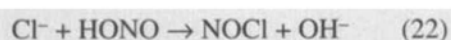
Fig. 6. Typical continuous flow experiment of ClONO<sub>2</sub> on ice at 180 K using a 4-mm-diameter-aperture Knudsen reactor at a flow rate of  $1.0 \cdot 10^{15}$  molecules s<sup>-1</sup>

concentration. It is in marked contrast to most reactants such as HCl whose solubility in H<sub>2</sub>SO<sub>4</sub> dramatically decreases with increasing H<sub>2</sub>SO<sub>4</sub> concentration. Our resulting  $\gamma$  values are significantly lower than the ones recently obtained by Leu and coworkers, the reason for which is unclear [25]. When we bring HCl to interact with a HONO-saturated H<sub>2</sub>SO<sub>4</sub>/H<sub>2</sub>O solution we measure low uptake coefficients  $\gamma$  on the order of 10<sup>-3</sup> or less, also in distinct contrast to results recently published which are in the range between 10<sup>-2</sup> and 10<sup>-1</sup>. However, if we measure the heterogeneous interaction of concurrent flows of HONO and HCl on ice we observe large  $\gamma$

values ranging from 0.07 at 180 K to 0.03 at 200 K thus showing a slight negative temperature dependence. The heterogeneous reaction is driven by the dissolution of HCl in ice and the formation of a liquid layer on the ice surface. HONO is taken up in a reversible process in less than a monolayer quantity on pure ice in the absence of HCl, whereas it interacts quite efficiently on a fluid layer containing HCl. Experimental data show conclusively that the uptake of HONO is strongly, and that of HCl somewhat enhanced in each other's presence.

This result may have far-reaching consequences as far as atmospheric implica-

tions in relation to air traffic are concerned, but it also seems to weaken the importance of this chlorine activation scheme on  $\text{H}_2\text{SO}_4$  aerosols of the global background atmosphere contrary to the conclusions spelled out in [25]. However, only model calculations approaching atmospheric conditions in their degree of realism may be able to assess the real significance of these experimental results including the weak interaction of NOCl with  $\text{H}_2\text{SO}_4$  solutions displayed in Fig. 8. Once again, the operating mechanism may be described as a nucleophilic substitution reaction involving the displacement of  $\text{OH}^-$  by  $\text{Cl}^-$ :



Apparently, this  $\text{S}_{\text{N}}2$ -type displacement reaction is a much more facile process than the corresponding  $\text{S}_{\text{N}}1$ -type reaction (Eqn. 23) which may even point to an inhibiting effect of  $\text{H}_2\text{SO}_4$  rather than a catalytic one:



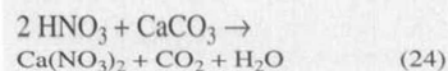
we, therefore, conclude that the chlorine activation scheme proposed by *Burley* and *Johnston* may not occur on catalytic surfaces such as  $\text{H}_2\text{SO}_4$  aerosols but rather in a direct way on ice particles.

### 3.5. The Reaction of $\text{HNO}_3$ with $\text{CaCO}_3$

Due to the corrosive nature of the polluted atmosphere, many monuments containing  $\text{CaCO}_3$ , including marble, sand-

stone and calcareous stone, are badly damaged. This fact has been summarily attributed to exposure to acid rain. However, even parts of monuments and statues that were never directly exposed to precipitation sometimes show roughly the same degree of damage. The incidence of episodes where acid fog or acidified aerosols are in contact with those monuments is highly variable and does not represent a coherent explanation for the damages incurred. Therefore, gas-phase pollutants have been searched for which model calculations predict to be ten times as efficient as acid precipitation because of longer contact/exposure times. We assumed that  $\text{HNO}_3$  may play the role of the gas-phase corroding agent because it is a reservoir compound for  $\text{NO}_x$  that is in steady increase in polluted urban atmospheres in view of the increasing emission strength of  $\text{NO}_x$ -releasing sources such as fossil fuel combustion. Gas-phase  $\text{HNO}_3$  does not possess acidic character and is characterized by a weak  $\text{HO}-\text{NO}_2$  bond of 50 kcal/mol.

The experiments show the rapid uptake of  $\text{HNO}_3$  and an equally as rapid formation of  $\text{H}_2\text{O}$  and  $\text{CO}_2$  when a  $\text{HNO}_3$  flow is exposed to powdered  $\text{CaCO}_3$ . It demonstrates conclusively that an acid-base reaction is occurring between  $\text{HNO}_3$  and the ionic calcite surface [26]:



However, the generation of  $\text{H}_2\text{O}$  and  $\text{CO}_2$  desorbing from the powdered sample hints at a complex mechanism possibly involving a precursor because of their delayed formation. Once steady state has been reached we observe complete mass balance between  $\text{HNO}_3$  consumed and  $\text{CO}_2$  generated. In separate reference experiments it was established that  $\text{H}_2\text{O}$  interacted with the calcite powder so that the incomplete mass balance for  $\text{H}_2\text{O}$  can be explained by incomplete desorption of the  $\text{H}_2\text{O}$  primary product. The surprise lies in the fact that the reaction according to Eqn. 24 seems to be quite an efficient hydrolysis reaction despite the 'dry' nature of the reaction system and is characterized by a reactive uptake coefficient for  $\text{HNO}_3$  on the order of  $\gamma = 0.10$ . Part of the explanation for such a large value of  $\gamma$  certainly lies in the 'sticky' nature of  $\text{HNO}_3$  whose tendency for adsorption on a variety of surfaces is well known. The pertinent description for the surface reactivity of  $\text{HNO}_3$  follows the *Langmuir-Hinshelwood* model of heterogeneous catalysis, wherein adsorbed  $\text{HNO}_3$  moves to active surface sites

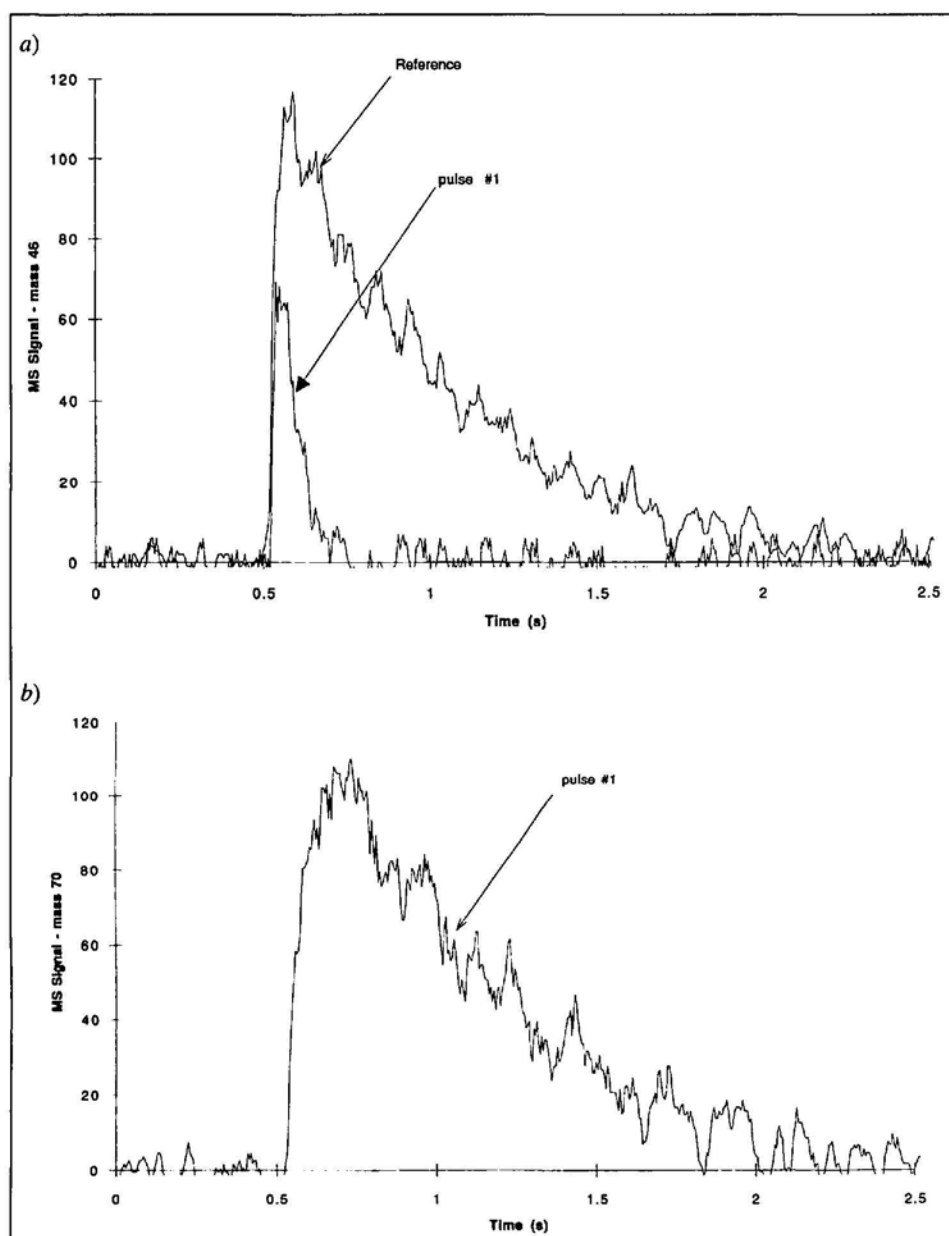


Fig. 7 a) Pulsed dosing experiment of  $\text{ClONO}_2$  on ice previously exposed to  $\text{HCl}$  at 200 K at a dose of  $\text{ClONO}_2$  of  $1.0 \cdot 10^{14}$  molecules corresponding to 10% of a formal monolayer. The mass-spectrometric trace displays  $m/e = 46$  ( $\text{NO}_2^+$ ) as a marker for the time dependent density of  $\text{ClONO}_2$  effusing out of the reactor. b) Same experiment as in Fig. 7a except that  $\text{Cl}_2$  is recorded as a function of time



by surface diffusion without ever desorbing [11].

### 3.6. The Reaction of N-Containing Oxides, Acids and Anhydrides with Salt Surfaces

90% of the world population lives in coastal areas which include a strip of land along the ocean's coastlines 100 km wide. These population centers generate massive amounts of air pollution which forms acids and oxidants such as tropospheric (surface) ozone in photochemical smog episodes which deteriorate the air quality to a significant extent. The OH free radical, mainly generated from photolysis of ozone and subsequent reaction with H<sub>2</sub>O vapor plays a central role in ozone formation which is just a by-product of NO<sub>x</sub>-catalyzed slow hydrocarbon oxidation (combustion) processes supported by photochemistry. This dark flame atmospheric process is comparable to internal combustion of fossil fuels with the main difference being that in combustion the free radicals necessary for maintaining the flame are generated in thermal dissociation processes, whereas they are generated mostly from photolytic processes in the atmosphere. When such heavily polluted urban air masses interact with the marine aerosol hovering above the coastline qualitatively new chemistry is occurring. Of prime interest is the question to what extent the normal chain carrier OH may be replaced by atomic chlorine whose reactivity is a factor of 20 larger than that of OH as far as chain-initiating H-abstraction reactions are concerned [27]. In addition, salt aerosol may also be found in the stratosphere after major volcanic eruptions which propel their ejecta up into the lower stratosphere to heights of just under 20 km.

We recently embarked on a program to systematically study the heterogeneous reactivity of NO<sub>x</sub>, HNO<sub>3</sub>, N<sub>2</sub>O<sub>5</sub>, ClONO<sub>2</sub>, and ClNO<sub>2</sub> on NaCl and KBr which are two important constituents of sea salt [28–30]. Some of the reactions and their products are the following:

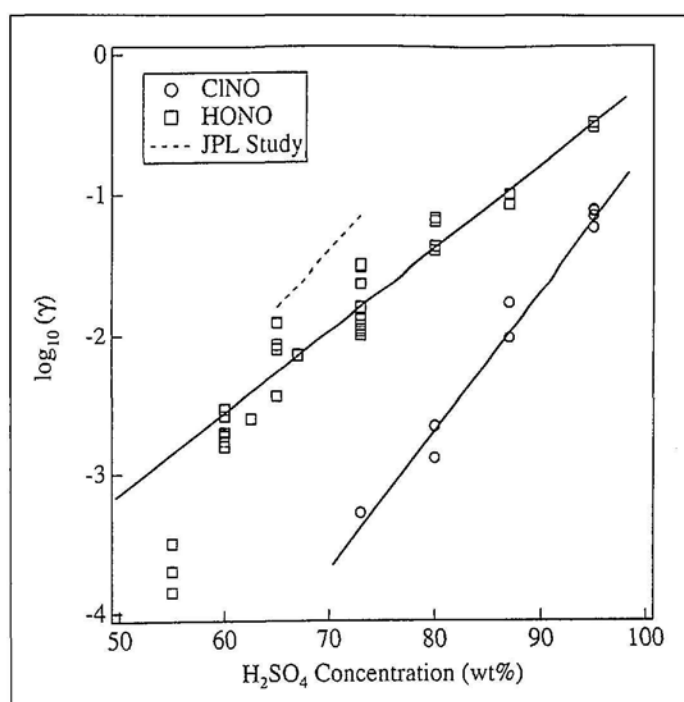
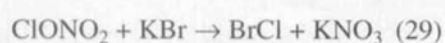
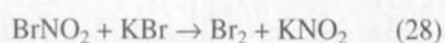


Fig. 8. A semi-logarithmic plot of the determined uptake probabilities for HONO and ClNO as a function of H<sub>2</sub>SO<sub>4</sub> concentration in the temperature range 215–273 K. The vapor pressure was balanced by an external flow of H<sub>2</sub>O.

Eqn. 25 corresponds to a simple exchange reaction in which volatile HNO<sub>3</sub> is exchanged for HCl. The Table displays the results for the measured uptake coefficients when gas-phase HNO<sub>3</sub> interacts with a salt sample that is presented either as a finely ground powder, as salt grains or as a thin film of several mg of mass and several μm of thickness. The Table shows that the uptake coefficient for HNO<sub>3</sub> on salt is invariant of the sample presentation: identical values of γ are obtained for exposure on a single crystal flat and on finely ground powder, two sample presentations which differ greatly with respect to their internal surface. The reason for this behavior lies in the fact that HNO<sub>3</sub> is known to be a 'sticky' compound which mainly stays on the external surface and thereby 'ignores' deeper layers of the sample as it never diffuses into the powder. This behavior is in marked contrast to the heterogeneous interaction of N<sub>2</sub>O<sub>5</sub> with salts, Eqns. 26 and 27, which is immeasurably small for a polished single crystal flat. The Table displays the results which are of the same magnitude as in the case of HNO<sub>3</sub> when the sample is presented in a form which gives the N<sub>2</sub>O<sub>5</sub> an opportunity to explore the internal surface of the sample. In this case the gas penetrates into the bulk and the measured uptake coefficient becomes dependent on the sample mass, thus of the number of grain layers. N<sub>2</sub>O<sub>5</sub> behaves like an ideal gas which does not stick to the sample surface and interacts with the chemical conversion sites on the salt sample from the gas phase by multiple adsorption-desorption steps. The corrected results for γ displayed in the Table

reduce the observed uptake coefficient to a per collision basis on a single layer of salt following a pore diffusion model proposed by Keyser and coworkers [31].

The primary reaction product BrNO<sub>2</sub> in Eqn. 27 was not directly monitored in view of its fast secondary reaction according to Eqn. 28. However, we observed its hydrolysis product HONO which forms with traces of moisture in the salt sample, whereas NO<sub>2</sub>Cl generated according to Eqn. 26 is kinetically stable under our conditions. An important switch in chemical reactivity takes place in going from ClONO<sub>2</sub> to BrNO<sub>2</sub>. The first corresponds to the formal anhydride of HNO<sub>3</sub> (N(+5)) and HCl (Cl(-1)), whereas the latter represents the formal anhydride of HONO (N(+3)) and HOBr (Br(+1)). The fast secondary reaction given by Eqn. 28 is, therefore, due to the change of oxidation state of the bromine in BrNO<sub>2</sub> compared to the chlorine in ClONO<sub>2</sub>.

In summary, we learned two important things from this systematic study: a) reactions according to Eqns. 26–30 all generate active halogen that is readily photolyzable in the daylight atmosphere thus supplying free radical-chain carriers for atmospheric oxidation processes, and b) we are able to distinguish 'sticky' from 'non-sticky', that is ideal gas, compounds in their heterogeneous interaction on salt. This is an important contribution to the ongoing discussion whether or not sample porosity has an effect on the determination of kinetic parameters of the heterogeneous interaction on frozen surfaces such as ices. The main result from the data presented in the Table can be summarized

Table. Synopsis of Uptake Coefficients  $\gamma$  [%] of Atmospherically Relevant Gases on Salt. The corrections to the observed uptake coefficients were performed according to [31].

Gas	Salt	Powder	Corr.	Grain	Corr.	Spray
ClNO <sub>2</sub>	KBr	1.9 ± 0.5	0.03 ± 0.02	0.08–0.7	0.015	0.007 ± 0.004
ClONO <sub>2</sub>	NaCl	24 ± 5	–	18 ± 4	–	28 ± 6
ClONO <sub>2</sub>	KBr	33 ± 5	–	36 ± 10	–	36 ± 10
HNO <sub>3</sub>	NaCl	2.8 ± 0.5	–	–	–	1.3 ± 0.8
HNO <sub>3</sub>	KBr	2.8 ± 0.5	–	4.7 ± 0.6	–	1.7 ± 0.8
N <sub>2</sub> O <sub>5</sub>	NaCl	3.0 ± 0.5	0.17	5–27	0.2	0.5 ± 0.2
N <sub>2</sub> O <sub>5</sub>	KBr	5.5 ± 0.1	0.35	25–58	0.4	0.3 ± 0.2

that  $\gamma$  not only depends on the properties of the substrate but also on the gas. In our case N<sub>2</sub>O<sub>5</sub> and ClNO<sub>2</sub> behave as ideal (non-sticky) gases whose heterogeneous interaction depends on the porosity of the substrate, whereas ClONO<sub>2</sub> and HNO<sub>3</sub> are sticky gases that do not penetrate into the bulk and are stopped at the external surface. In these latter two cases porosity is not an issue with respect to their interaction with salt which presents an ideal training ground for exploring aspects of sample porosity because their presentation is easily controlled at ambient temperature.

#### 4. Concluding Remarks

We have seen that many different areas of physical chemistry contribute to the study of heterogeneous chemistry such as chemical reaction kinetics, the theory of gas kinetics, thermochemistry, material properties (phase diagrams), vacuum technology and inorganic/organic synthesis, to name just a few. It is our opinion that this field is quickly moving across traditional scientific disciplines as it already includes aspects of atmospheric physics and meteorology, which makes this field so fascinating. The interaction with biology and the biosphere, oceanography and other fields of the earth sciences may loom just around the corner.

We set out to elucidate the *mechanistic* implications of heterogeneous reactions in order to provide the correct chemistry that goes into a model which may be fit for reliable projections into the future behavior of the atmosphere. It is impossible to reproduce realistic atmospheric conditions in the laboratory because the concentrations are often too low, the particle growth rates and the associated time scales too long. However, with an understanding of the *mechanism* we may be able to extrapolate from laboratory conditions to the atmosphere in order to reconcile and interpret field observations which may then

be used to validate atmospheric chemistry models.

I would like to express my sincere gratitude to Prof. H. van den Bergh for having given me the opportunity to conduct these studies in his laboratory and for his continuing support of the tasks still lying ahead of us. I have also benefitted from his insights as well as from his lively interest in the progress of the scientific enterprise. My thanks go also to the sponsors of this research at *Fonds National Suisse de la Recherche Scientifique*, the *Office Fédéral de l'Éducation et de la Science* (OFES) and the *Office Fédéral de l'Environnement, Forêt et Paysage* (OFEFP) for their generous financial support. I would like to thank my many collaborators who contributed to the undisputable success of the Laboratoire de Pollution Atmosphérique et Sol since its inception in 1991 and without whom none of these experimental investigations would have been possible. My thanks go to Arnaud Allanic, Talis Bauer, François Caloz, Agostino Clericetti, Fred F. Fenter, Lukas Gutzwiller, Raoul Oppliger, Marçal Pires, Kevin D. Tabor, Axel Thielmann, Wang Wei, and Matthias Wolf. I also would like to acknowledge the efforts of our Italian mastercraftsman Flavio Comino for whom no task as daunting as it may seem was and is impossible.

Received: March 14, 1996

- [1] J.C. Farman, B.G. Gardiner, J.D. Shanklin, *Nature (London)* **1985**, 315, 207.
- [2] J.G. Anderson, 'Free Radicals in the Earth's Atmosphere: Their Measurement and Interpretation', *Ann. Rev. Phys. Chem.* **1987**, 38, 489.
- [3] 'Atmospheric Ozone 1985', World Meteorological Organization (WMO) Global Ozone Research and Monitoring Project - Report No. 16, produced by NASA, FAA, NOAA, UNEP, WMO, EC and BMFT. See page 46 and 132.
- [4] 'The Probable Role of Stratospheric 'Ice' Clouds: Heterogeneous Chemistry of the 'Ozone Hole'', M.J. Molina, in 'The Chemistry of the Atmosphere: Its Impact on Global Change', Ed. J.G. Calvert, Blackwell Scientific Publications, Oxford, UK, 1994.
- [5] L.T. Molina, M.J. Molina, *J. Phys. Chem.* **1987**, 91, 433.
- [6] 'Scientific Assessment of Ozone Depletion: 1994', World Meteorological Organization Global Ozone Research and Monitoring Project - Report No. 37, produced by NOAA, NASA, UNEP and WMO.
- [7] 'The Changing Ozone Layer', R.D. Bojkov, World Meteorological Organization (WMO) and United Nations Environment Programme (UNEP), 1995.
- [8] G. Baumbach, 'Luftreinhaltung', 3rd edn., Springer Verlag, Berlin - Heidelberg - New York, 1994.
- [9] 'Le Réchauffement Planétaire et la Suisse: Bases d'une Stratégie Nationale', Office Fédéral de l'Environnement, des Forêts et du Paysage (OFEFP), CH-3003 Berne. Rapport du Groupe de Travail Interdépartemental sur l'Evolution du Système Climatique, Berne, janvier 1994.
- [10] 'AERONOX. The Impact of NO<sub>x</sub> Emissions from Aircraft upon the Atmosphere at Flight Altitudes 8–15 km'. Ed. U. Schumann, EC-DLR Publication on Research related to Aeronautics and Environment, August 1995.
- [11] 'Dynamic Heterogeneous Catalysis', Ed. K. Tamaru, Academic Press, London - New York - San Francisco, 1978.
- [12] D.M. Golden, G.N. Spokes, S.W. Benson, *Angew. Chem.* **1973**, 14, 602.
- [13] J. Marti, K. Mauersberger, *Geophys. Res. Lett.* **1993**, 20, 363.
- [14] D.R. Haynes, N.J. Tro, S.M. George, *J. Phys. Chem.* **1992**, 96, 8502.
- [15] L. Gutzwiller, K.D. Tabor, M.J. Rossi, *J. Phys. Chem.* **1996**, submitted.
- [16] 'The Probable Role of Stratospheric 'Ice' Clouds: Heterogeneous Chemistry of the 'Ozone Hole'', M.J. Molina, in 'The Chemistry of the Atmosphere: Its Impact on Global Change', Ed. J. Calvert, Blackwell Scientific Publications, Oxford, 1994.
- [17] A. Thielmann, L. Gutzwiller, M.J. Rossi, 1996, in preparation.
- [18] J.P.D. Abbatt, K.D. Beyer, A.F. Fucaloro, J.R. McMahon, P.J. Wooldridge, R. Zhang, M.J. Molina, *J. Geophys. Res.* **1992**, 97(D14), 15819.
- [19] D.R. Hanson, A.R. Ravishankara, *J. Phys. Chem.* **1992**, 96, 2682.
- [20] J.R. Sodeau, A.B. Horn, S.F. Banham, Th.G. Koch, *J. Phys. Chem.* **1995**, 99, 6258.
- [21] R. Oppliger, A. Allanic and M.J. Rossi, *J. Phys. Chem.* **1996**, submitted.
- [22] R. Zhang, J.T. Jayne, M.J. Molina, *J. Phys. Chem.* **1994**, 98, 867.
- [23] J.D. Burley, H.S. Johnston, *Geophys. Res. Lett.* **1992**, 19, 1359, 1363.
- [24] F.F. Fenter, M.J. Rossi, *J. Phys. Chem.* **1996**, in press.
- [25] R. Zhang, L.F. Keyser, M.T. Leu, *J. Phys. Chem.* **1996**, 100, 339.
- [26] F.F. Fenter, F. Caloz, M.J. Rossi, *Atmos. Environ.* **1995**, 22, 3365.
- [27] R. Atkinson, D.L. Baulch, R.A. Cox, R.F. Hampson, Jr., J.A. Kerr, M.J. Rossi, J. Troe, *J. Phys. Chem. Ref. Data* **1996**, in press.
- [28] F.F. Fenter, F. Caloz, M.J. Rossi, *J. Phys. Chem.* **1994**, 98, 9801.
- [29] F.F. Fenter, F. Caloz, M.J. Rossi, *J. Phys. Chem.* **1996**, 100, 1008.
- [30] F. Caloz, F.F. Fenter, M.J. Rossi, *J. Phys. Chem.* **1996**, 100, in press.
- [31] L.T. Chu, M.-T. Leu, L.F. Keyser, *J. Phys. Chem.* **1993**, 97, 12798.